Long-lived coupled peeling ballooning modes preceding ELMs on JET

C. Perez von Thun,[1,2] L. Frassinetti,[3] L. Horvath,[4] S. Saarelma,[5] L. Meneses,[6] E. de la Luna,[7] M. Beurskens,[8] J. Boom,[9] J. Flanagan,[5] J.C. Hillesheim,[5] C.F. Maggi,[5] S.J.P. Pamela,[5] E.R. Solano,[7] and JET Contributors‡

[1]Forschungszentrum Jülich GmbH, Institut für Energie- und Klimaforschung - Plasmaphysik, 52425 Jülich, Germany.
[2]EUROfusion PMU, Culham Science Centre, Abingdon, OX14 3DB, United Kingdom.
[3]Department of Fusion Plasma Physics, Royal Institute of Technology KTH, Stockholm, Sweden.
[4]York Plasma Institute, University of York, Heslington, York, YO10 5DD, UK
[5]Culham Centre for Fusion Energy, Abingdon, OX14 3DB, UK.
[6]Instituto de Plasmas e Fusão Nuclear, Instituto Superior Técnico, Universidade de Lisboa, 1049-001 Lisboa, Portugal.
[7]Laboratorio Nacional de Fusion, CIEMAT, E-28040, Madrid, Spain.
[8]Max-Planck-Institut für Plasmaphysik, Wendelsteinstr. 1, D-17491 Greifswald, Germany.
[9]Max-Planck-Institut für Plasmaphysik, Boltzmannstr. 2, D-85748 Garching, Germany.

E-mail: christian.perezvonthun@euro-fusion.org

Abstract. In some JET discharges, type-I Edge Localised Modes (ELMs) are preceded by a class of low frequency oscillations [Perez et al Nucl. Fusion 44 (2004) 609]. While in many cases the ELM is triggered during the growth phase of this oscillation, it is also observed that this type of oscillations can saturate and last for several tens of ms until an ELM occurs. In order to identify the nature of these modes, a wide pre-ELM oscillation database including detailed pedestal profile information has been assembled and analysed in terms of MHD stability parameters. The existence domain of these pre-ELM oscillations and the statistical distribution of toroidal mode numbers (n) up to $n = 16$ has been mapped in ballooning alpha (α_{ball}) and either edge current density (J_{edge}) or pedestal collisionality ($\nu^*_{ee,ped}$) coordinates and compared to linear MHD stability predictions. The pre-ELM oscillations are reliably observed when the J/α ratio is high enough for the pedestal to access the coupled peeling-ballooning (PB) domain (aka stability nose). Reversely, when the pedestal is found to be in or near the high-n ballooning domain (which is at low J/α ratio), ELMs are usually triggered promptly, i.e. with no detectable pre-ELM oscillations, or with pre-ELM oscillations only observable on ECE whose n appears to be too high to be resolved by the magnetics. Individual discharges can sometimes exhibit a fairly wide range of pre-ELM mode numbers, but for a wider database the statistical n-number domains are found to be well ordered along the J-α stability boundary and behave as expected from PB theory: the higher the J/α ratio, the lower the mode's measured n tends to be. Within the measurement uncertainties, the measured n is usually found to be compatible with the most unstable n predicted by the linear stability code MISHKA1. These results confirm the earlier hypothesis that these modes are coupled peeling-ballooning modes, and extend and generalise to higher mode numbers the work by Huysmans

‡ See the author list of "X. Litaudon et al 2017 Nucl. Fusion 57 102001".

et al [Nucl. Fusion 38 (1998) 179], who identified the lowest n modes as pure external kink modes. Since the destabilisation of PB modes is widely accepted to give rise to ELMs, the mode saturation and delayed ELM triggering that is sometimes observed is rather unexpected. Possibilities to reconcile the extended lifetime of these modes with current ELM models are briefly discussed but will require further investigation.

PACS numbers: 52.35.Py, 52.55.Tn

Submitted to: *Nucl. Fusion*

1. Introduction

The edge region of high confinement ('H-mode') [1] tokamak plasmas has a strong influence on the fusion performance of the tokamak as a whole. A narrow boundary layer with reduced transport ('pedestal') [2] develops with steep density and temperature gradients that can drive a variety of macroscopic instabilities. The increase in plasma stored energy is limited by the onset of periodic bursts called Edge Localised Modes (ELMs) [3–9], each of which leading to a transient collapse of the pedestal. Understanding these modes is imperative for correctly predicting fusion performance and controlling ELMs in ITER [10, 11].

The most widely accepted model to explain the occurrence of ELMs is the peeling ballooning (PB) model [12–14] . According to this model, ELMs are triggered by the destabilisation of coupled PB modes, which were first theoretically predicted by Connor and Wilson [15].

The body of literature testing the validity of the PB model is vast. The main lines of investigation have focused on the study of pre-ELM pedestal profiles and ELM characteristics in detail. This includes the ELMs' dominant mode numbers and ELM filament dynamics [16–28], pedestal height and width scalings (e.g. [29]), the comparison of measured pedestal profiles with linear MHD stability code predictions (e.g. [30–35]), and non-linear modelling (e.g. [36–44]). Also, the PB model is used as one of the constraints in the predictive pedestal model EPED [45,46], which has been used to predict the limiting pressure pedestal height and width for several present tokamaks, with overall good success (e.g. [32, 46–48]). On JET, the EPED model works quite well at low gas fuelling, but not so well at high gas rates [49–55].

The search for the PB modes has also motivated the study of electromagnetic fluctuation activity arising near the plasma periphery prior to ELMs. These have been observed on a number of tokamaks and can be broadly classified into two categories: (a) Quasi-coherent fluctuations which are present during a large fraction of the inter-ELM period and are often seen to influence the pedestal profile evolution between ELMs [56–64]. These are transport phenomena that have been linked with kinetic ballooning mode (KBM) or micro-tearing mode (MTM) activity, rather than PB modes. (b) Lower frequency more coherent fluctuations which arise closer to the ELM event (often dubbed pre-ELM oscillations or "precursors") [28, 57, 63, 65–70]. On JET, both types of activity, (a) and (b), are present and clearly distinguishable from each other [56], but this paper is only devoted to the latter. One example is shown in figure 1.

Empirically, the low frequency ($\lesssim$20kHz) oscillations regularly precede type I ELM crashes in some, but not all, discharges on JET [66]. They have only been seen in connection with type I ELMs, never with type III ELMs. The range of toroidal mode numbers n reported so far was 1-13, but in this paper this range is extended to $n = 16$. The poloidal mode number m could be determined in dedicated studies for modes with lowest $n = 1$ [71, 72]. Those cases typically yielded m values of order 4 or 5, which is consistent with the edge localisation of these modes. The pre-ELM oscillations are localized close to the plasma boundary, and are most well observed on the optically thick ECE channels in the inner half of the steep gradient region of the pedestal [66]. Further out ECE is no longer used because it becomes optically thin, but reflectometry still works there and also detects the modes in the outer part

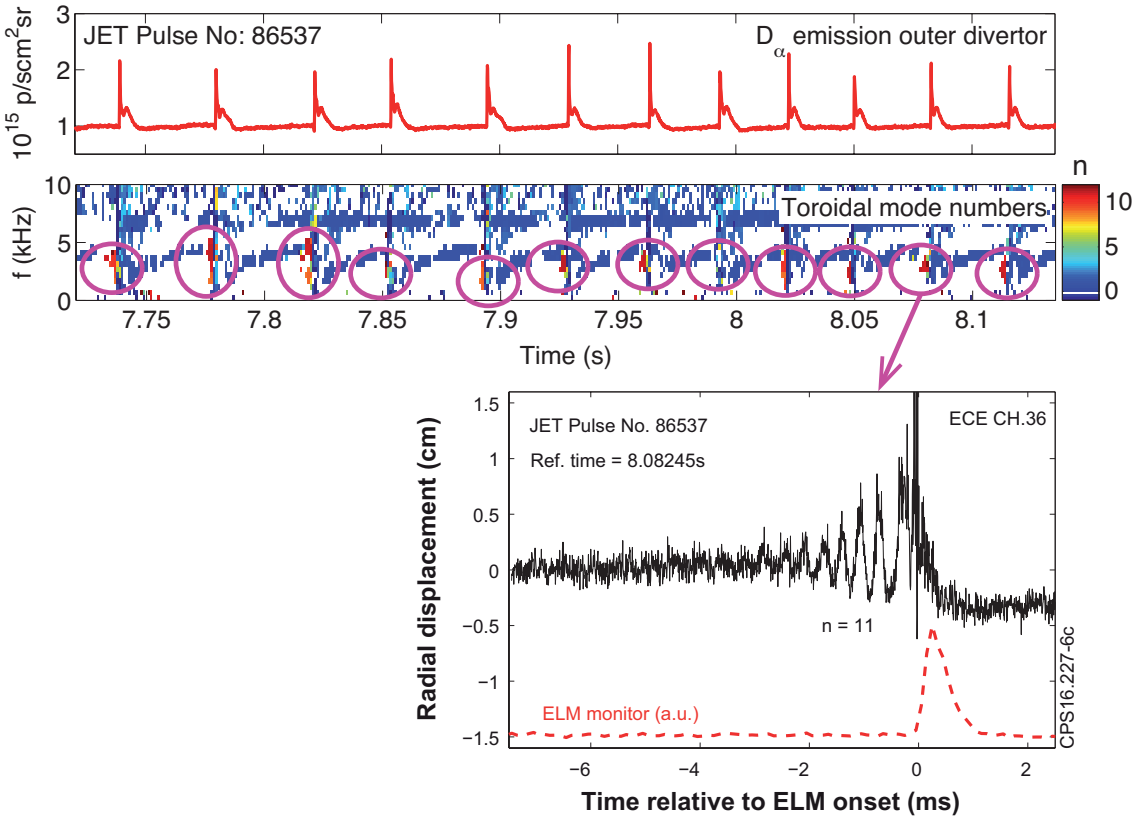

Figure 1. Example of a time window where ELMs are systematically preceded by the low frequency pre-ELM oscillations (the mostly red-ish spots encircled in magenta, denoting toroidal mode numbers n = 9-12, inferred from magnetics). Shown below is a zoomed view for one of the pre-ELM oscillations with $n = 11$, giving the radial displacement amplitude evolution measured with an ECE channel in the steep region of the pedestal. Typically, the radial displacement associated with these modes as seen by both reflectometry and ECE is of order few mm up to 1cm. For comparison, the pressure pedestal width for JET H-modes is of order 2cm.

of the steep gradient region and bottom of the pedestal. Typically, the radial displacement associated with these modes as seen by both reflectometry and ECE on the outboard side of the plasma is of order few mm up to 1cm , with associated uncertainties for ECE of order 30% and for reflectometry of order 10-20%. For comparison, the pressure pedestal width on JET is of order 2cm. Mutichannel O-mode reflectometry also shows the radial mode structure of the pre-ELM oscillations exhibits no radial phase inversions from inside the pedestal all the way up to the separatrix and beyond, so they have kink parity, not tearing parity [66]. Also the array of ECE channels, which does not reach all way to the separatrix (because of loss of optical thickness) but compared to the O-mode reflectometer has better coverage for radial locations inwards of the pedestal, shows no radial phase inversions.

Identification of the nature of these modes was so far largely prevented by the limited edge profile information available. Making use of improved edge profile diagnostics, the work presented here closes this gap by systematically analysing the lower frequency type pre-ELM

MHD fluctuation measurements of the pedestal, for a wide operational range, and comparing the results with stability modelling predictions. Experimentally, we will limit ourselves in this article to modes with $n \leq 16$, which is the highest n that is still resolvable by the mode number reconstruction algorithm deployed here. However, it should not be implied that this is the highest mode number that is actually present at JET. In fact, we have found some instances where pre-ELM oscillations could be detected on edge ECE only, not on magnetics, especially at high collisionality. Presumably, these are modes with even higher n, but this remains to be proven.

To our knowledge, this is the first time that data are combined and analysed in such a way and over a large database. The methods used for this will be explained in section 2. This section gives information about the database itself, which diagnostics are included, and about the choice of coordinates used to analyse the database in stability space. It also discusses the validity of approximations, and which bootstrap current models and simulation codes are used. The main results of our analysis will be presented in section 3, including the extent of the domain in stability space covered by the database, in which parts of the domain the pre-ELM oscillations can be detected, and how the toroidal mode numbers of pre-ELM oscillations are distributed in stability space and compare with modelling.

2. Methodology

An extensive database has been compiled comprising 460 deuterium type-I ELMy H-mode discharge flat tops, including discharges run with either a CFC-based or a Be/W-based (ITER-like) first wall, with and without oscillations. It covers a wide range of operating parameters, i.e. plasma current (I_p =1.3-4.5 MA), toroidal field (B_0 =1.7-3.6T), edge safety factor (q_{95} =2.6-4.8), plasma shape (δ = 0.19-0.47), heating (P_{aux} =4-27MW) and fuelling rates. From this, one can expect to obtain a fully representative dataset for the pre-ELM conditions in J-α space that are or have been routinely accessed on JET since 2008.

The database combines electron density (n_e) and temperature (T_e) profiles from high resolution Thomson Scattering (HRTS) with fast fluctuation data from Mirnov coils and electron cyclotron emission (ECE) to find the modes. A toroidal array of Mirnov coils is used to infer the toroidal mode number n of the pre-ELM oscillations during the discharge flat top. Mode numbers can sometimes vary from ELM to ELM. If more than one mode number is observed, all n numbers are recorded in the database and equally asigned to this discharge flat top. A single representative pre-ELM profile is assigned to the whole flat top of a discharge. To obtain this profile, HRTS profile data during the last 30% of an ELM cycle has been averaged over several ELM cycles during the flat top and fitted with a modified hyperbolic tangent [73, 74]. Due to instrument vignetting, for some (older) parts of the database only pedestal top values are available.

The analysis is done in terms of dimensionless, MHD relevant variables. For the pressure drive of ballooning modes, we have approximated the maximum normalised pressure gradient (ballooning alpha, $\alpha = -(2\mu_0 R q^2/B^2) dp/dr$ [75]), i.e. the maximum reached across the pedestal radial profile, as $\widehat{\alpha}_{\mathrm{KBM}} = -2\mu_0 R p'_{\mathrm{KBM}} q_{95}^2/B_0^2$, with $p'_{\mathrm{KBM}} = c(1 +$

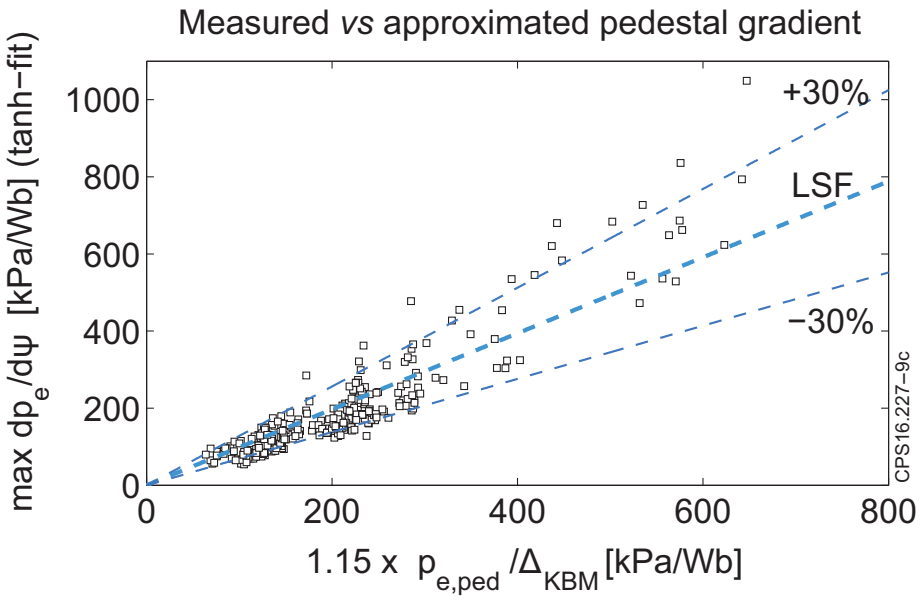

Figure 2. Comparison of maximum pedestal electron pressure gradient extracted from (pre-ELM) tanh-fitted profiles (y-axis) with a KBM-based approximation formula that relies on pedestal top measurements only (x-axis), using a set of 350 discharges covering a large range of discharge conditions (shape, heating, etc). For this wide set of data, a least squares fit (LSF) standard deviation of 24% is obtained.

$\gamma_i) n_{e,ped} T_{e,ped} / \Delta_{\mathrm{KBM}}$. Here, R is the major radius, q_{95} is the safety factor at 95% of normalised flux, B_0 is the magnetic field on axis, $\gamma_i(Z_{\mathrm{eff}}) < 1$ accounts for the main ion dilution by impurities, the subscript "ped" denotes the pedestal top value, $\Delta_{\mathrm{KBM}} = 0.076 \beta_{\mathrm{pol,ped}}^{1/2}$ is a kinetic ballooning mode (KBM) based scaling for the pedestal width [46] and $c = 1.15$ is a constant empirical fit factor. This assumes $T_{i,ped}$=$T_{e,ped}$, which for the plasma boundary region is a good approximation. Thus, the maximum pedestal pressure gradient in the α formula is replaced with an easier to measure "pedestal top/KBM width" based approximation, that only requires measurements at the pedestal top. Dedicated scans on JET have revealed cases where the pedestal width is not well described by a KBM scaling [52, 53, 55]. Despite that, comparing this approximation with the fitted profile gradients of 350 discharges yields only a moderate standard deviation of 24% (figure 2).

The boostrap current [76] typically dominates in the edge region. Hence, as a proxy for the normalised current drive $J_{||}/J_{\mathrm{av}}$, the flux surface averaged bootstrap current density computed by the first principles kinetic code NEO [77, 78] is used, specifically its peak value reached across the pedestal radial profile, $<J_{||,\mathrm{BS}} B>_{\mathrm{max}} / B_0$ (for brevity, $J_{||,\mathrm{BS}}^{\mathrm{NEO}}$) which is then normalised against the average current density flowing in the plasma (i.e. $J_{\mathrm{av}} = I_p/A$, with A the area of the plasma poloidal cross-section). We use NEO rather than the Sauter formula [79, 80] , which has been also often used in literature, because the database covers a wide range of pedestal collisionalities and the Sauter formula has been found to overestimate the bootstrap current at high collisionality [81]. (This latter point is also clearly visible in figure 3.)

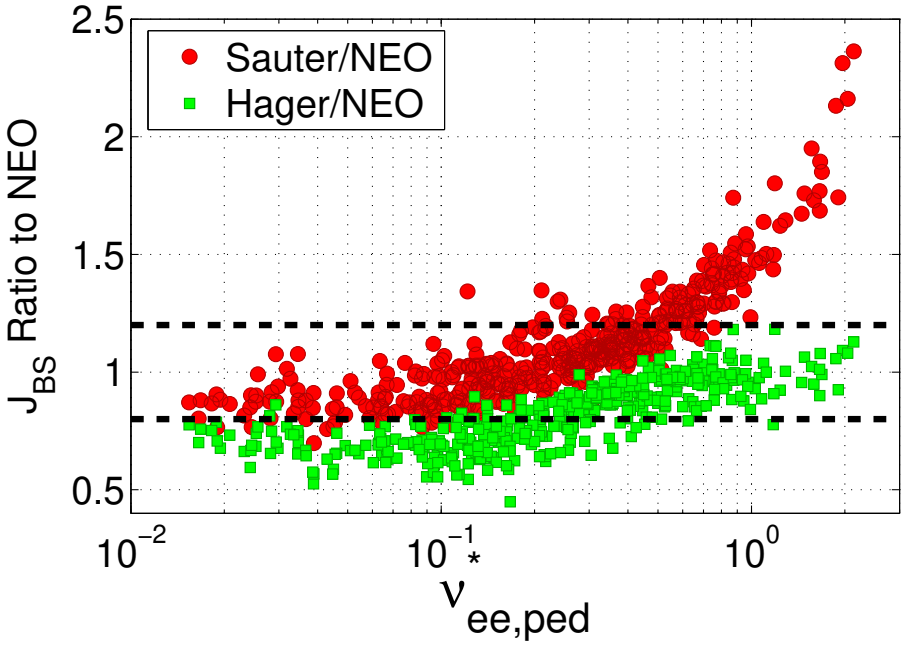

Figure 3. Comparison of bootstrap analytic formulas to NEO for a subset of the database, as a function of normalised pedestal top collisionality (e-e). The y-axis denotes the ratio of the bootstrap current profile maximum values predicted by either Sauter (circles) or Hager formulas (squares) relative to the NEO profile peak prediction. The dashed lines denote the boundaries for $\pm 20\%$ deviation from 1.

One difficulty is that NEO is presently not coupled to the HELENA fixed boundary equilibrium code [82], which produces the input for the MHD stability calculations. Hence, for the MHD stability calculations the NEO prediction is approximated with the help of two analytical formulas: the Sauter formula for low collisionality pedestals ($\nu^*_{\rm ee,ped} <\sim 0.3$) and the Hager formula [83] for high collisionality pedestals ($\nu^*_{\rm ee,ped} >\sim 0.4$). Around $\nu^*_{\rm ee,ped} = 0.3$-0.4, whichever of the two formulas is closer to NEO is used. By proceeding in this way, it is possible to approximate the NEO value analytically to better than 20% accuracy across the entire range of collisionalities in our database, as shown in figure 3. The MHD stability calculations themselves are computed by the linear finite-n MHD code MISHKA1 [84].

The ratio of the two driving forces, J vs α, is determined by the pedestal collisionality. This is because the boostrap current is roughly proportional to the pressure gradient, but is reduced by collisions. As the collisionality is reduced, more current is produced at a given pressure gradient. Hence, the collisionality determines where the PB boundary is met, as illustrated in the cartoon of figure 4. Specifically, for a measure of the J/α ratio we use here the normalised neoclassical electron-electron collisionality at the pedestal top, $\nu^*_{\rm ee,ped} = Rq_{95}\epsilon^{-3/2}/\lambda_{\rm ee}$, with $\lambda_{\rm ee} = 1.47\times10^{23}\, T^2_{\rm e,ped}/(n_{\rm e,ped}\ln\Lambda)$, ϵ is the inverse aspect ratio and $ln\Lambda$ is the Coulomb logarithm. Figure 4 plots the J/α ratio against $\nu^*_{\rm ee,ped}$, confirming the validity of this choice. Figure 4 also quantifies how wide the range of J/α ratios covered by the database is. Considering only the bootstrap current contribution, it covers a (very

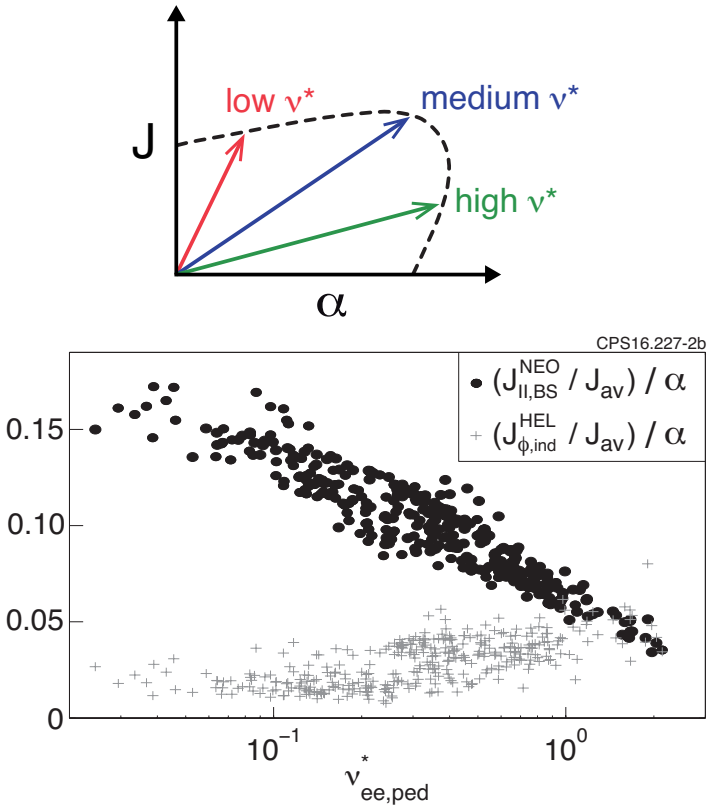

Figure 4. (Top) Cartoon showing how the pedestal collisionality influences the J/α ratio in the pedestal and hence determines where the PB boundary (dashed line) is met. (Bottom) Dependence of normalised J/α ratio on the normalised (e-e) pedestal top collisionality, distinguishing between the bootstrap contribution (computed by NEO, circles) and the inductive current contribution (computed by HELENA, crosses). The main conclusion is that $\nu^*_{\rm ee,ped}$ serves as a good measure of the J/α ratio, and that the database covers a wide range of J/α ratios.

significant) factor 4-5 variation between lowest and highest collisionalities, and therefore we can expect the ensemble of datapoints to be scattered along the PB stability boundary over an extended range, all the way from current dominated (peeling driven) conditions to pressure dominated (ballooning driven) conditions.

Figure 4 also includes the toroidal Ohmic current contribution $J_{\phi,\rm ind}$ at the radial location of the maximum bootstrap current, equally normalised, from a separate computation with the HELENA code. It has some tendency to increase at high collisionality, but overall the Ohmic contribution has a more flat dependence on $\nu^*_{\rm ee,ped}$. So, in first approximation we can consider it introduces simply a constant offset and the trend for the overall edge current to decrease with collisionality remains valid.

3. Main results

Figure 5 plots the full database (460 datapoints) in $\widehat{\alpha}_{\rm KBM}$-$\nu^*_{\rm ee,ped}$ space, distinguishing between low triangularity (LT) and high triangularity (HT) of the poloidal plasma cross section.

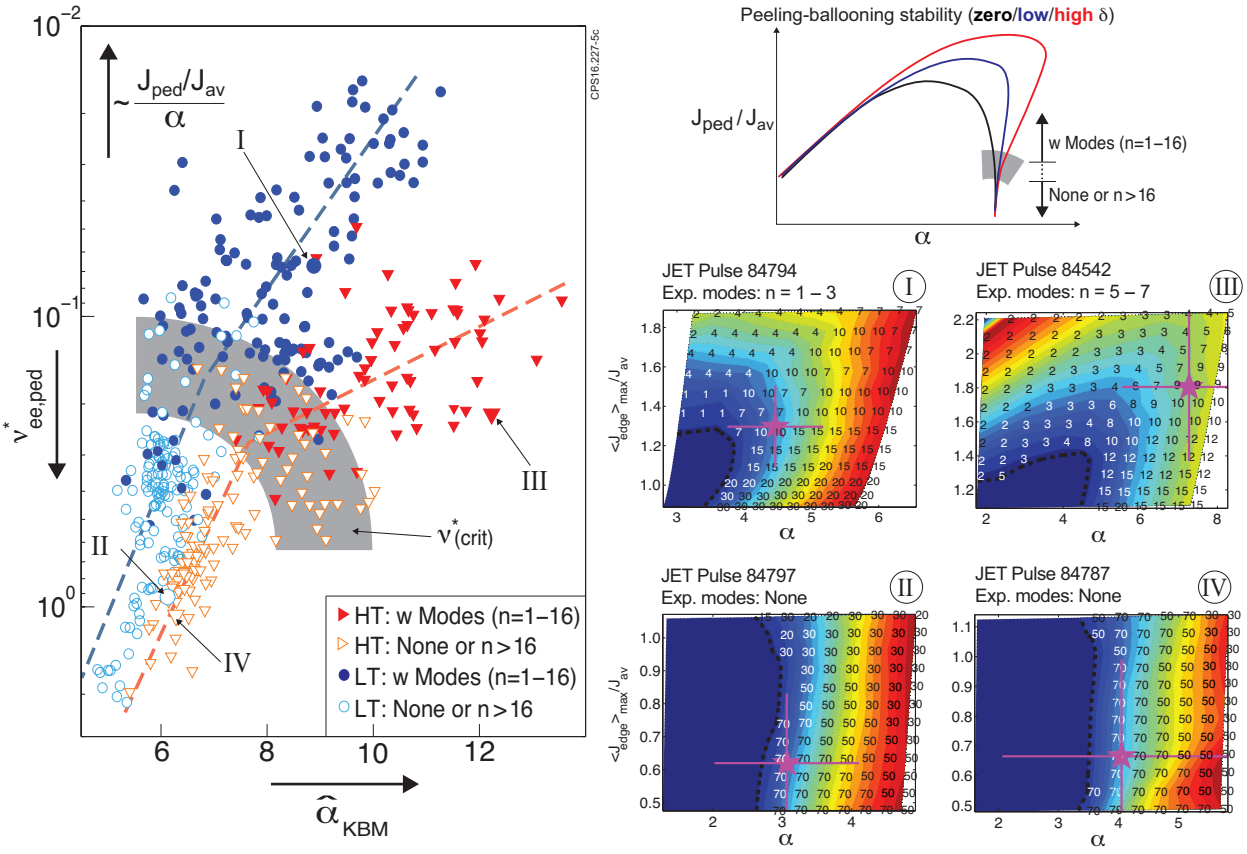

Figure 5. (Left:) Existence domain of cases with (full symbols) and without modes (open symbols) up to $n = 16$, in $\widehat{\alpha}_{\mathrm{KBM}}$-$\nu^*_{\mathrm{ee,ped}}$ coordinates, distinguishing high ($0.33 < \delta < 0.47$, triangles) and low ($0.19 < \delta < 0.31$, circles) plasma triangularity. Notice in this plot the collisionality (y-axis) direction is inverted, increasing from top to bottom. The lines and shaded transition area are to guide the eye, with colours matching the adjacent PB stability cartoon (top right). MISHKA stability calculations for four discharges (see labels I-IV on left) are shown underneath. Here, the overlaid numbers indicate the most unstable n numbers predicted in stability space (font colour choice for legibility), background shade denotes growth rate (increases from blue to red) and the operational point with estimated uncertainty is shown in magenta. For comparison, information on the experimentally observed modes for each of the four cases is included in the titles. It should be noted that MISHKA uses a different formula for α (we use HELENA definition), hence α absolute values do not coincide with left plot. In the MISHKA plots, the edge current includes the inductive contribution, and the bootstrap contribution was computed using analytical approximation formulas which agree with NEO to within 20%.

Triangularity is well known to be a key player for ballooning stability, expanding the stable region as sketched in the adjacent cartoon. It can be seen that the dataset splits into two distinct domains: At low edge current (high $\nu^*_{\mathrm{ee,ped}}$, or low J/α ratio), LT (circles) and HT (triangles) datapoints run approximately parallel (same α increase for given reduction in $\nu^*_{\mathrm{ee,ped}}$, i.e. increase in $J_{||}/J_{\mathrm{av}}$). This is the domain of the "pure" ballooning mode (no peeling component). On the other hand, at low $\nu^*_{ee,ped}$ (high J/α ratio), both groups of datapoints diverge, such that, for a given increase in edge current density, the α increase

is more pronounced at high shaping. The transition between the two regimes marks the grey shaded region highlighted in the neighbouring cartoon, which is the only part of the PB stability diagram where this bifurcation behaviour occurs§, and is empirically found to happen in JET around a "critical" collisionality, $\nu^*_{\text{ee,ped}}(crit)$, of ~ 0.15-0.3.

This interpretation is confirmed by stability calculations with the MHD code MISHKA1, done for selected discharges above and below the critical collisionality, using analytical edge current approximations close to the NEO prediction (as described in section 2). For discharges with collisionality above $\nu^*_{\text{ee,ped}}(crit)$, MISHKA predicts these to be in or near the domain susceptible to high n 30-70 pure ballooning instabilities, whereas for discharges with collisionality below $\nu^*_{\text{ee,ped}}(crit)$, MISHKA predicts these to be near the PB stability nose, where $n \leq 15$ modes are predicted. Four cases along both extremes are shown in sub-figures I-IV of figure 5.

From the cartoon in figure 5, one would expect to observe a reduction in α if the discharge crosses the current (peeling) limit well away from the PB nose. Instead, the database shows that most (if not all) of the ELMs on JET are triggered either towards the pressure limited side of the stability diagram, or near the PB nose, but not deeper towards the current (peeling) limited side. The data in figure 5 shows no clear reduction of the achieved α even at the lowest collisionalities (J/α ratios). This is also consistent with MISHKA, as we have not found any cases for which MISHKA finds the operational point in the peeling limit region well away from the PB nose.

Importantly, figure 5 also distinguishes between cases with pre-ELM oscillations up to $n = 16$ (full symbols) and without pre-ELM oscillations (open symbols), or at least no modes with resolvable n up to $n = 16$, as discussed in the introduction. The pre-ELM mode activity is reliably observed only for $\nu^*_{\text{ee,ped}} < \nu^*_{\text{ee,ped}}(crit)$, i.e. when discharges approach the PB nose, while for $\nu^*_{\text{ee,ped}} > \nu^*_{\text{ee,ped}}(crit)$ (the pure ballooning region) it is generally not detected. Near the transition region, $\nu^*_{\text{ee,ped}} \sim \nu^*_{\text{ee,ped}}(crit)$, either case can be found. So, we find that the mode occurrence is as sketched by the arrows in the cartoon on the top right.

As mentioned earlier, the toroidal mode number n of the pre-ELM oscillations has been reconstructed for every discharge in the database using an array of toroidally distributed magnetic pick-up coils. One can group all discharges exhibiting a particular mode number n, and the resulting dataset for that n then forms a "cloud" in J-α space. The distribution of the different n number clouds is plotted in figure 6, again using approximate $\widehat{\alpha}_{\text{KBM}}$-$\nu^*_{\text{ee,ped}}$ coordinates and distinguishing between LT and HT. Despite the heterogeneity of the database, the mode number domains are almost perfectly sorted, going from high to low n along the pre-ELM boundary with decreasing collisionality, i.e. increasing J/α ratio. The overlap between domains is real as often several modes with different n co-exist in the plasma. The observed ordering follows PB mode expectations: increasing edge current density is stabilising for ballooning modes (high n) and destabilising for peeling modes (lower n). The ordering is preserved when plotting the measured mode number domains in true J-α, full

§ The reader can easily convince himself that the mentioned bifurcation in J vs α space (the coordinates of the cartoon) equally exists in J/α vs α space (the coordinates of the left plot). Plotting in J/α vs α space will merely accentuate the bifurcation further.

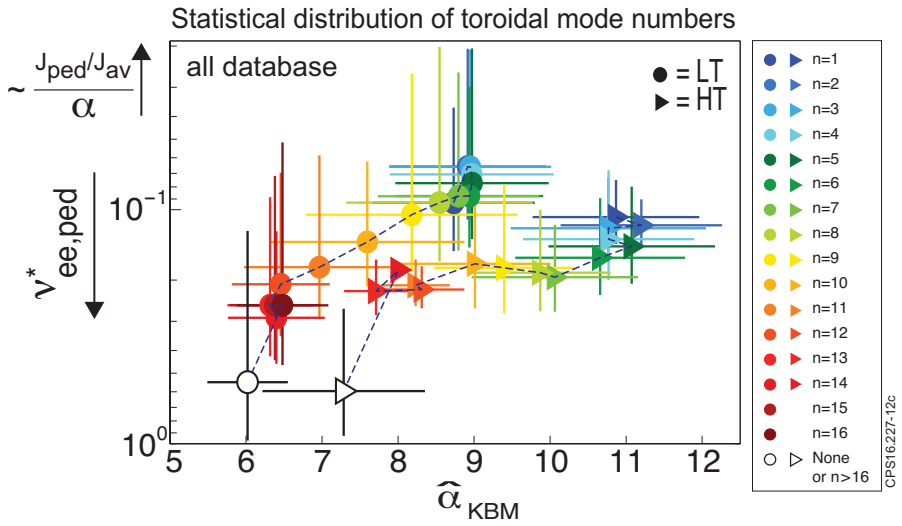

Figure 6. Occurrence domains of measured mode numbers n, using the approximated pedestal top-based coordinates $\widehat{\alpha}_{\mathrm{KBM}}$-$\nu^*_{\mathrm{ee,ped}}$ already used in figure 5. Notice the collisionality (y-axis) direction is inverted, increasing from top to bottom. Each mode number is represented with a different colour, and we distinguish again between LT cases (circles), and HT cases (triangles). For each n, the symbol marks the statistical center of the domain (average coordinate of the datapoints) and the size of the bars shows the extent of the domain (standard deviation of datapoints from the domain center), which is not to be confused with the measurement uncertainty. The dashed lines connect neighbouring mode numbers within LT and HT. Notice that mode number domains are almost perfectly ordered, going from high to low n along the pre-ELM boundary with decreasing collisionality, i.e. increasing J/α ratio.

HRTS-profile based (so not KBM-approximated), stability coordinates, as shown in figure 7, showing again that this is not artefact due to our particular choice of coordinates. Also, the limited size of the bars in J-α space for such a diverse database demonstrates these coordinates are succesfully capturing the physics of these modes.

In addition to plasma shaping, it is also known that beta has a stabilising effect on PB modes [85]. Figure 8 shows the mode number domains for the high triangularity branch of figure 6, separately for plasmas with low and high poloidal beta. The beta expansion effect manifests itself through the shift of the domains towards higher α with increasing beta. Note the statistical n numbers domains shift "rigidly" and their ordering along the boundary is maintained. This behaviour is again in line with PB mode expectations: For a given shape, the n number remains primarily determined by the J/α ratio (i.e. by the collisionality), hence by where the PB boundary is met (cf also with cartoon in figure 4).

A 1:1 comparison of the experimentally observed toroidal mode numbers with the most unstable n values predicted by MISHKA has also been attempted. This requires a good understanding of the uncertainties involved, which are not all well known. Nevertheless, a limited comparison is possible. To this end, we selected a set of 18 discharges scanning from low to high collisionality at low and high shaping whose HRTS data was subjected to an even more meticulous analysis for best possible profile accuracy and statistical error information. This set includes the four examples I-IV shown in figure 5. Assuming that NEO yields a good

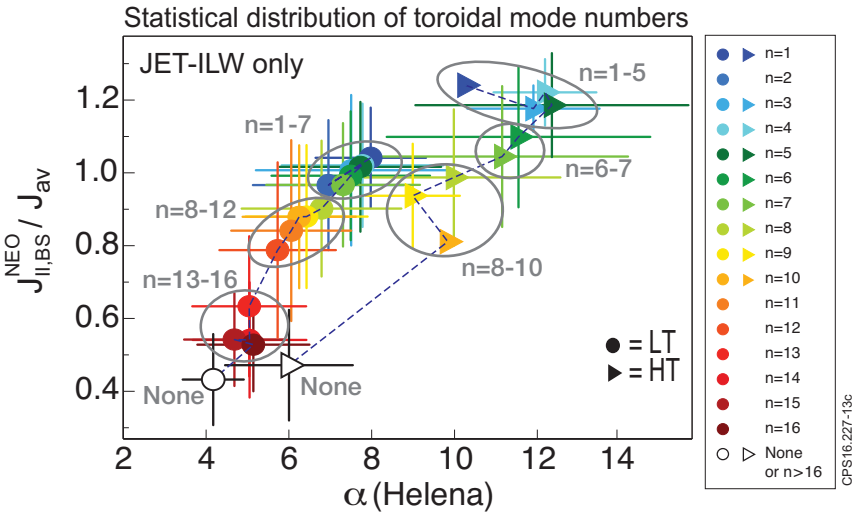

Figure 7. Same as figure 6, but now the measured mode number domains are shown using full profile, code computed J-α stability coordinates based on the HRTS profiles (J computed by NEO, and α computed by HELENA). Compared to figure 6, this uses only a subset of the database with full profiles information available (i.e. HRTS profiles not affected by diagnostic vignetting, as discussed in the introduction). Notice also the rather limited extent of each n domain (size of bars) in J-α coordinates, despite the heterogeneity of the database.

approximation of the actual edge current density in the plasma, and that the overall error is dominated by the profile gradient determination, we find that in 16 out of 18 cases MISHKA is consistent with the experiment, while in 2 cases MISHKA predicts a higher n. E.g. a case with good agreement is subfigure III of figure 5, where the experimental mode numbers 5-7 feature among the most unstable ones predicted by MISHKA within the J-α uncertainty, whereas subfigure I of figure 5 shows one of the cases with not so good agreement (here the observed $n = 1$-3 modes are seen to be most unstable only just outside the uncertainty area). It is worth noting that if we just consider n values at the nominal operational point (star-symbol), we find that there is a general tendency for MISHKA to give a higher estimate than seen in experiment. Also, it has been generally noticed in the past that for JET plasmas MISHKA almost never predicts operational points accessing the lowest $n < 3$ (kink) domain. One possible explanation for these two observations could be edge velocity shear, which has not been included in the MISHKA calculations and is known to be destabilising for low n kink modes [86].

4. Discussion

In this work we have exploited diagnostic enhancements to improve the characterisation of a class of low frequency edge localised pre-ELM oscillations on JET for toroidal mode numbers up to $n = 16$. The method is based on the construction of a broad database combining fluctuation and pedestal profile information and the application of various techniques for estimating stability parameters, which are by themselves also valuable. To our knowledge,

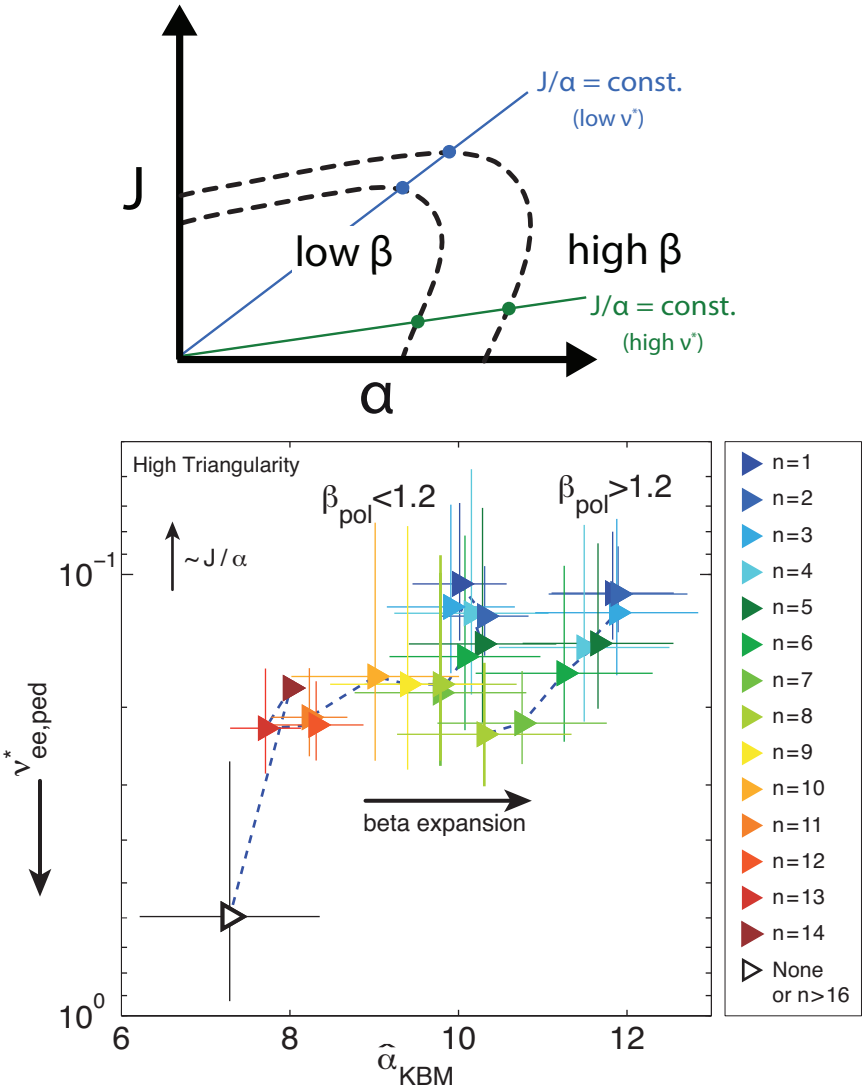

Figure 8. (Top) Cartoon illustrating the well known stabilising effect of beta on PB modes. Note for a given J/α ratio, the PB boundary is met at higher α when beta increases. (Bottom) High triangularity branch as from figure 6, but now additionally distinguishing between low and high poloidal beta discharges. Note the domains shift to higher α with beta, but the observed n numbers remain primarily determined by the J/α ratio (i.e. the pedestal collisionality), so by where the PB boundary is met relative to the PB nose.

this type of approach has not been attempted yet on other machines. With this, the existence domain of the pre-ELM oscillations and the statistical distribution of toroidal mode numbers has been mapped in ballooning alpha (α) and either edge current density (J_{edge}) or pedestal collisionality ($\nu^*_{e,ped}$) coordinates and compared to linear MHD stability predictions. They are encountered only at sufficiently high J_{edge}/α ratio and in particular in the J-α domain expected for PB modes but not pure ballooning modes. The balance of J and α for a given shape and/or poloidal beta determines their mode number with n as expected from PB mode theory, with n clearly observed statistically to increase with decreasing J. Furthermore, the oscillations can reach radial displacement amplitudes of a significant fraction of the pedestal

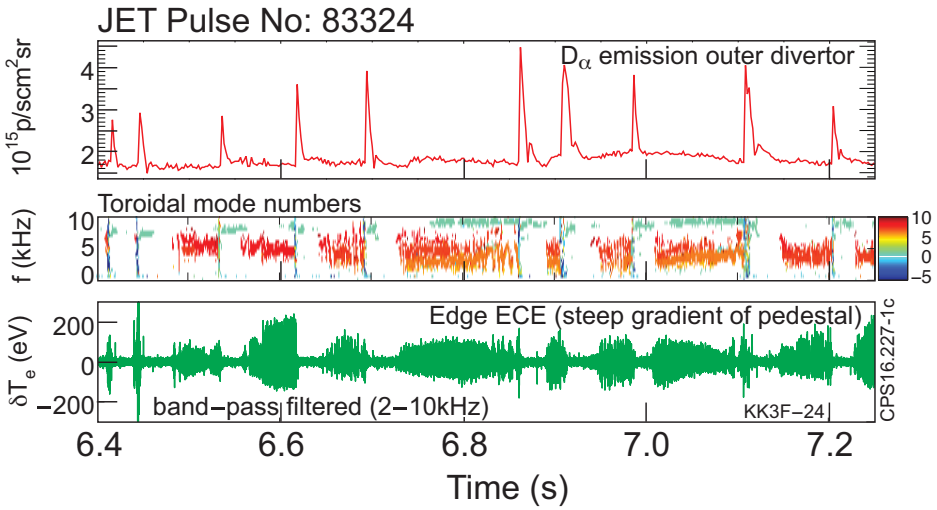

Figure 9. Example for saturated pre-ELM oscillations persisting for several tens of ms until eventually an ELM is triggered. The pre-ELM oscillations are the orange/red coloured bands (denoting toroidal mode number n = 6-8, inferred from magnetics), and the edge ECE channel shows how the amplitude of the corresponding temperature fluctuations is evolving.

width. Together with earlier findings: (a) they rotate in the ion (not electron) diamagnetic direction and the radial mode structure of these oscillations has kink (not tearing) parity [66] , and (b) the lowest n modes have been identified as external kink modes through analysis of 2D Soft X-Ray data [71] , it is justified to identify the pre-ELM oscillations as coupled PB ballooning modes with gradual transition into pure peeling modes with decreasing mode number. Also, magnetics see increasing inboard/outboard (ballooning) amplitude asymmetry with increasing mode number which are at least consistent with this identification, but here radial damping in-/out-asymmetries also need to be considered [66].

The ELM triggering causality has not been addressed in detail here, and this should be the subject of future studies. The observation of increased ELM triggering likelyhood during the growth phase of the pre-ELM oscillation illustrated in figure 1 corroborates that there is a causal relationship between the onset of these modes and the ELM. This is in line with current ELM models that predict the ELM to be triggered by PB modes, and in line with the predictive pedestal model EPED, that uses the PB boundary as a constraint to predict the pedestal height. But sometimes the oscillations can saturate in amplitude without an obvious explanation and last for several tens of ms before an ELM crash is triggered. An example of this behaviour is shown in figure 9. One possibility for the different non-linear behaviour is that the strong velocity shear that is known to exist in the pedestal region delays the ELM onset, by trapping the mode filaments inside the separatrix [8]. Rotational shear has also been proposed to explain the saturation of Edge Harmonic Oscillations [87–89] in Quiescent H-mode (QH-mode) plasma regime [90], for which there is strong evidence that these are nonlinearly saturated external kink modes. It would be significant if this mechanism is not unique to low n but also occurs for all measured n up to $n = 16$. This will require further investigation.

The population of pre-ELM datapoints below the bifurcation in figure 5 shows unequivocally that ELMs on JET can be triggered also in the domain of high n pure ballooning modes, well away from the PB nose. This implies that on JET the high-n boundary does not act merely as a pedestal gradient limiting "soft" boundary, as sometimes proposed (e.g. in [14]).
The ability to detect coupled peeling ballooning modes in experiment enables ways to further refine ELM physics models. Some questions that could be more easily addressed are: how does the pedestal pass through marginal stability, which is something that the predictive pedestal model EPED does not directly address; is the ELM triggered by the coupled PB mode itself or by a secondary instability facilitated by the PB mode (e.g. a non-linear high-n ballooning mode [91, 92]); does the mode number and mode width of the PB mode have an impact on the size of the ELM crash [12].
In addition, they can be used as an extra source of information to constrain linear and non-linear MHD simulations of ELMs, e.g. by tweaking the starting equilibrium within the measurement uncertainties to ensure that the experimentally observed toroidal mode number is reproduced in the early stages of the ELM crash simulation.

Acknowledgments

This work has been carried out within the framework of the EUROfusion Consortium and has received funding from the Euratom research and training programme 2014-2018 under grant agreement No 633053. The views and opinions expressed herein do not necessarily reflect those of the European Commission.

References

[1] F. Wagner, G. Becker, K. Behringer, D. Campbell, A. Eberhagen, W. Engelhardt, G. Fussmann, O. Gehre, J. Gernhardt, G. v. Gierke, G. Haas, M. Huang, F. Karger, M. Keilhacker, O. Klüber, M. Kornherr, K. Lackner, G. Lisitano, G. G. Lister, H. M. Mayer, D. Meisel, E. R. Müller, H. Murmann, H. Niedermeyer, W. Poschenrieder, H. Rapp, H. Röhr, F. Schneider, G. Siller, E. Speth, A. Stäbler, K. H. Steuer, G. Venus, O. Vollmer, and Z. Yü. Regime of improved confinement and high beta in neutral-beam-heated divertor discharges of the asdex tokamak. *Phys. Rev. Lett.*, 49:1408–1412, Nov 1982.

[2] Hajime Urano. Pedestal structure in h-mode plasmas. *Nuclear Fusion*, 54(11):116001, 2014.

[3] H. Zohm. Edge localized modes (elms). *Plasma Physics and Controlled Fusion*, 38(2):105, 1996.

[4] J. W. Connor. Edge-localized modes - physics and theory. *Plasma Physics and Controlled Fusion*, 40(5):531, 1998.

[5] J. W. Connor. A review of models for elms. *Plasma Physics and Controlled Fusion*, 40(2):191, 1998.

[6] W Suttrop. The physics of large and small edge localized modes. *Plasma Physics and Controlled Fusion*, 42(5A):A1, 2000.

[7] H R Wilson, S C Cowley, A Kirk, and P B Snyder. Magneto-hydrodynamic stability of the h-mode transport barrier as a model for edge localized modes: an overview. *Plasma Physics and Controlled Fusion*, 48(5A):A71, 2006.

[8] A. Kirk, D. Dunai, M. Dunne, G. Huijsmans, S. Pamela, M. Becoulet, J. R. Harrison, J. Hillesheim, C. Roach, and S. Saarelma. Recent progress in understanding the processes underlying the triggering of and energy loss associated with type i elms. *Nuclear Fusion*, 54(11):114012, 2014.

[9] A. W. Leonard. Edge-localized-modes in tokamaks. *Physics of Plasmas*, 21(9):090501, 2014.

[10] A. Loarte, G. Huijsmans, S. Futatani, L. R. Baylor, T. E. Evans, D. M. Orlov, O. Schmitz, M. Becoulet, P. Cahyna, Y. Gribov, A. Kavin, A. Sashala Naik, D. J. Campbell, T. Casper, E. Daly, H. Frerichs, A. Kischner, R. Laengner, S. Lisgo, R.A. Pitts, G. Saibene, and A. Wingen. Progress on the application of elm control schemes to iter scenarios from the non-active phase to dt operation. *Nuclear Fusion*, 54(3):033007, 2014.

[11] G. T. A. Huijsmans, C. S. Chang, N. Ferraro, L. Sugiyama, F. Waelbroeck, X. Q. Xu, A. Loarte, and S. Futatani. Modelling of edge localised modes and edge localised mode control. *Physics of Plasmas*, 22(2):021805, 2015.

[12] P. B. Snyder, H. R. Wilson, J. R. Ferron, L. L. Lao, A. W. Leonard, T. H. Osborne, A. D. Turnbull, D. Mossessian, M. Murakami, and X. Q. Xu. Edge localized modes and the pedestal: A model based on coupled peelingballooning modes. *Physics of Plasmas*, 9(5):2037–2043, 2002.

[13] H. R. Wilson et al. Ideal magnetohydrodynamic stability of the tokamak high-confinement-mode edge region. *Physics of Plasmas*, 6(5):1925–1934, 1999.

[14] J. W. Connor, R. J. Hastie, H. R. Wilson, and R. L. Miller. Magnetohydrodynamic stability of tokamak edge plasmas. *Physics of Plasmas*, 5(7):2687–2700, 1998.

[15] J. W. Connor and H. R. Wilson. Ideal mhd stability at the plasma edge. In J. W.Connor, E. Sindoni, and J. Vaclavik, editors, *ISPP-17 Piero Caldirola*, Theory of Fusion Plasmas, pages 441–446, SIF, Bologna, 1996.

[16] A. Kirk, H. R. Wilson, G. F. Counsell, R. Akers, E. Arends, S. C. Cowley, J. Dowling, B. Lloyd, M. Price, and M. Walsh. Spatial and temporal structure of edge-localized modes. *Phys. Rev. Lett.*, 92:245002, Jun 2004.

[17] A Kirk, H R Wilson, R Akers, N J Conway, G F Counsell, S C Cowley, J Dowling, B Dudson, A Field, F Lott, B Lloyd, R Martin, H Meyer, M Price, D Taylor, M Walsh, and the MAST team. Structure of elms in mast and the implications for energy deposition. *Plasma Physics and Controlled Fusion*, 47(2):315, 2005.

[18] A Kirk, N Ben Ayed, G Counsell, B Dudson, T Eich, A Herrmann, B Koch, R Martin, A Meakins, S Saarelma, R Scannell, S Tallents, M Walsh, H R Wilson, and the MAST team. Filament structures at the plasma edge on mast. *Plasma Physics and Controlled Fusion*, 48(12B):B433, 2006.

[19] A Kirk, T Eich, A Herrmann, H W Muller, L D Horton, G F Counsell, M Price, V Rohde, V Bobkov, B Kurzan, J Neuhauser, H Wilson, the ASDEX Upgrade, and MAST Teams. The spatial structure of type-i elms at the mid-plane in asdex upgrade and a comparison with data from mast. *Plasma Physics and Controlled Fusion*, 47(7):995, 2005.

[20] R. Maingi, C.E. Bush, E.D. Fredrickson, D.A. Gates, S.M. Kaye, B.P. LeBlanc, J.E. Menard, H. Meyer, D. Mueller, N. Nishino, A.L. Roquemore, S.A. Sabbagh, K. Tritz, S.J. Zweben, M.G. Bell, R.E. Bell, T. Biewer, J.A. Boedo, D.W. Johnson, R. Kaita, H.W. Kugel, R.J. Maqueda, T. Munsat, R. Raman, V.A. Soukhanovskii, T. Stevenson, and D. Stutman. H-mode pedestal, elm and power threshold studies in nstx. *Nuclear Fusion*, 45(9):1066, 2005.

[21] J.L. Terry, I. Cziegler, A.E. Hubbard, J.A. Snipes, J.W. Hughes, M.J. Greenwald, B. LaBombard, Y. Lin, P. Phillips, and S. Wukitch. The dynamics and structure of edge-localized-modes in alcator c-mod. *Journal of Nuclear Materials*, 363-365:994 – 999, 2007. Plasma-Surface Interactions-17.

[22] A Kirk, N Asakura, J A Boedo, M Beurskens, G F Counsell, T Eich, W Fundamenski, A Herrmann, Y Kamada, A W Leonard, S Lisgo, A Loarte, N Oyama, R A Pitts, A Schmid, and H R Wilson. Comparison of the spatial and temporal structure of type-i elms. *Journal of Physics: Conference Series*, 123(1):012011, 2008.

[23] G. S. Yun, W. Lee, M. J. Choi, J. Lee, H. K. Park, B. Tobias, C. W. Domier, N. C. Luhmann, A. J. H. Donné, and J. H. Lee. Two-dimensional visualization of growth and burst of the edge-localized filaments in kstar h-mode plasmas. *Phys. Rev. Lett.*, 107:045004, Jul 2011.

[24] B Vanovac, E Wolfrum, S S Denk, F Mink, F M Laggner, G Birkenmeier, M Willensdorfer, E Viezzer, M Hoelzl, S J Freethy, M G Dunne, A Lessig, N C Luhmann Jr, the ASDEX Upgrade Team, and the EUROfusion MST1 Team. Effects of density gradients and fluctuations at the plasma edge on ecei measurements at asdex upgrade. *Plasma Physics and Controlled Fusion*, 60(4):045002, 2018.

[25] R.P. Wenninger, H. Zohm, J.E. Boom, A. Burckhart, M.G. Dunne, R. Dux, T. Eich, R. Fischer, C. Fuchs, M. Garcia-Munoz, V. Igochine, M. Hlzl, Luhmann N.C. Jr, T. Lunt, M. Maraschek, H.W. Mller, H.K. Park, P.A. Schneider, F. Sommer, W. Suttrop, E. Viezzer, and the ASDEX Upgrade Team. Solitary magnetic perturbations at the elm onset. *Nuclear Fusion*, 52(11):114025, 2012.

[26] R.P. Wenninger, H. Reimerdes, O. Sauter, and H. Zohm. Non-linear magnetic perturbations during edge-localized modes in tcv dominated by low n mode components. *Nuclear Fusion*, 53(11):113004, 2013.

[27] M. Rack, B. Sieglin, T. Eich, J. Pearson, Y. Liang, I. Balboa, S. Jachmich, A. Wingen, S.J.P. Pamela, and JET EFDA Contributors. Findings of pre-elm structures through the observation of divertor heat load patterns at jet with applied n=2 perturbation fields. *Nuclear Fusion*, 54(7):072004, 2014.

[28] K.E. Thome, M.W. Bongard, J.L. Barr, G.M. Bodner, M.G. Burke, R.J. Fonck, D.M. Kriete, J.M. Perry, J.A. Reusch, and D.J. Schlossberg. H-mode plasmas at very low aspect ratio on the pegasus toroidal experiment. *Nuclear Fusion*, 57(2):022018, 2017.

[29] P. A. Schneider, E. Wolfrum, R. J. Groebner, T. H. Osborne, M. N. A. Beurskens, M. G. Dunne, B. Kurzan, T. Ptterich, E. Viezzer, the ASDEX Upgrade Team, the DIII-D Team, and JET EFDA Contributors. Analysis of temperature and density pedestal gradients in aug, diii-d and jet. *Nuclear Fusion*, 53(7):073039, 2013.

[30] P. B. Snyder et al. Elms and constraints on the h-mode pedestal: peelingballooning stability calculation and comparison with experiment. *Nuclear Fusion*, 44(2):320, 2004.

[31] S. Saarelma et al. Mhd and gyro-kinetic stability of jet pedestals. *Nuclear Fusion*, 53(12):123012, 2013.

[32] R. J. Groebner et al. Improved understanding of physics processes in pedestal structure, leading to improved predictive capability for iter. *Nuclear Fusion*, 53(9):093024, 2013.

[33] A Pitzschke, R Behn, O Sauter, B P Duval, J Marki, L Porte, L Villard, S Yu Medvedev, and the TCV Team. Electron temperature and density profile evolution during the edge-localized mode cycle in ohmic and electron cyclotron-heated h-mode plasmas in tcv. *Plasma Physics and Controlled Fusion*, 54(1):015007, 2012.

[34] F.M. Laggner, E. Wolfrum, M. Cavedon, M.G. Dunne, G. Birkenmeier, R. Fischer, M. Willensdorfer, F. Aumayr, The EUROfusion MST1 Team, and The ASDEX Upgrade Team. Plasma shaping and its impact on the pedestal of asdex upgrade: edge stability and inter-elm dynamics at varied triangularity. *Nuclear Fusion*, 58(4):046008, 2018.

[35] Y F Wang, G S Xu, B N Wan, G Q Li, N Yan, Y L Li, H Q Wang, Y-K Martin Peng, T Y Xia, S Y Ding, R Chen, Q Q Yang, H Q Liu, Q Zang, T Zhang, B Lyu, J C Xu, W Feng, L Wang, Y J Chen, Z P Luo, G H Hu, W Zhang, L M Shao, Y Ye, H Lan, L Chen, J Li, N Zhao, Q Wang, P B Snyder, Y Liang, J P Qian, X Z Gong, and EAST team. Stability analysis of elms in long-pulse discharges with elite code on east tokamak. *Plasma Physics and Controlled Fusion*, 60(5):055002, 2018.

[36] P. B. Snyder, H. R. Wilson, and X. Q. Xu. Progress in the peeling-ballooning model of edge localized modes: Numerical studies of nonlinear dynamics. *Physics of Plasmas*, 12(5):056115, 2005.

[37] G.T.A. Huysmans and O. Czarny. Mhd stability in x-point geometry: simulation of elms. *Nuclear Fusion*, 47(7):659, 2007.

[38] X.Q. Xu, B.D. Dudson, P.B. Snyder, M.V. Umansky, H.R. Wilson, and T. Casper. Nonlinear elm simulations based on a nonideal peelingballooning model using the bout++ code. *Nuclear Fusion*, 51(10):103040, 2011.

[39] S J P Pamela, G T A Huysmans, M N A Beurskens, S Devaux, T Eich, S Benkadda, and JET EFDA contributors. Nonlinear mhd simulations of edge-localized-modes in jet. *Plasma Physics and Controlled Fusion*, 53(5):054014, 2011.

[40] S J P Pamela, G T A Huijsmans, A Kirk, I T Chapman, J R Harrison, R Scannell, A J Thornton, M Becoulet, F Orain, and the MAST Team. Resistive mhd simulation of edge-localized-modes for double-null discharges in the mast device. *Plasma Physics and Controlled Fusion*, 55(9):095001, 2013.

[41] M. Kim, M.J. Choi, J. Lee, G.S. Yun, W. Lee, H.K. Park, C.W. Domier, N.C. Luhmann Jr, X.Q. Xu, and the KSTAR Team. Comparison of measured 2d elms with synthetic images from bout++ simulation in kstar. *Nuclear Fusion*, 54(9):093004, 2014.

[42] F. Liu, G.T.A. Huijsmans, A. Loarte, A.M. Garofalo, W.M. Solomon, P.B. Snyder, M. Hoelzl, and L. Zeng.

Nonlinear mhd simulations of quiescent h-mode plasmas in diii-d. *Nuclear Fusion*, 55(11):113002, 2015.

[43] M. Bcoulet, M. Kim, G. Yun, S. Pamela, J. Morales, X. Garbet, G.T.A. Huijsmans, C. Passeron, O. Fvrier, M. Hoelzl, A. Lessig, and F. Orain. Non-linear mhd modelling of edge localized modes dynamics in kstar. *Nuclear Fusion*, 57(11):116059, 2017.

[44] F Liu, G T A Huijsmans, A Loarte, A M Garofalo, W M Solomon, M Hoelzl, B Nkonga, S Pamela, M Becoulet, F Orain, and D Van Vugt. Nonlinear mhd simulations of qh-mode diii-d plasmas and implications for iter high q scenarios. *Plasma Physics and Controlled Fusion*, 60(1):014039, 2018.

[45] P. B. Snyder, R. J. Groebner, A. W. Leonard, T. H. Osborne, and H. R. Wilson. Development and validation of a predictive model for the pedestal heighta). *Physics of Plasmas*, 16(5), 2009.

[46] P. B. Snyder, R. J. Groebner, J. W. Hughes, T. H. Osborne, M. Beurskens, A. W. Leonard, H. R. Wilson, and X. Q. Xu. A first-principles predictive model of the pedestal height and width: development, testing and iter optimization with the eped model. *Nuclear Fusion*, 51(10):103016, 2011.

[47] J.R. Walk, P.B. Snyder, J.W. Hughes, J.L. Terry, A.E. Hubbard, and P.E. Phillips. Characterization of the pedestal in alcator c-mod elming h-modes and comparison with the eped model. *Nuclear Fusion*, 52(6):063011, 2012.

[48] A Merle, O Sauter, and S Yu Medvedev. Pedestal properties of h-modes with negative triangularity using the eped-ch model. *Plasma Physics and Controlled Fusion*, 59(10):104001, 2017.

[49] M. N. A. Beurskens, L. Frassinetti, C. Challis, C. Giroud, S. Saarelma, B. Alper, C. Angioni, P. Bilkova, C. Bourdelle, S. Brezinsek, P. Buratti, G. Calabro, T. Eich, J. Flanagan, E. Giovannozzi, M. Groth, J. Hobirk, E. Joffrin, M. J. Leyland, P. Lomas, E. de la Luna, M. Kempenaars, G. Maddison, C. Maggi, P. Mantica, M. Maslov, G. Matthews, M.-L. Mayoral, R. Neu, I. Nunes, T. Osborne, F. Rimini, R. Scannell, E. R. Solano, P.B. Snyder, I. Voitsekhovitch, P. de Vries, and JET-EFDA Contributors. Global and pedestal confinement in jet with a be/w metallic wall. *Nuclear Fusion*, 54(4):043001, 2014.

[50] M N A Beurskens, J Schweinzer, C Angioni, A Burckhart, C D Challis, I Chapman, R Fischer, J Flanagan, L Frassinetti, C Giroud, J Hobirk, E Joffrin, A Kallenbach, M Kempenaars, M Leyland, P Lomas, G Maddison, M Maslov, R McDermott, R Neu, I Nunes, T Osborne, F Ryter, S Saarelma, P A Schneider, P Snyder, G Tardini, E Viezzer, E Wolfrum, the ASDEX Upgrade Team, and JET-EFDA Contributors. The effect of a metal wall on confinement in jet and asdex upgrade. *Plasma Physics and Controlled Fusion*, 55(12):124043, 2013.

[51] S. Saarelma, A. Jrvinen, M. Beurskens, C. Challis, L. Frassinetti, C. Giroud, M. Groth, M. Leyland, C. Maggi, J. Simpson, and JET Contributors. The effects of impurities and core pressure on pedestal stability in joint european torus (jet)a). *Physics of Plasmas*, 22(5), 2015.

[52] C. F. Maggi, S. Saarelma, F. J. Casson, C. Challis, E. de la Luna, L. Frassinetti, C. Giroud, E. Joffrin, J. Simpson, M. Beurskens, I. Chapman, J. Hobirk, M. Leyland, P. Lomas, C. Lowry, I. Nunes, F. Rimini, A.C.C. Sips, and H. Urano. Pedestal confinement and stability in jet-ilw elmy h-modes. *Nuclear Fusion*, 55(11):113031, 2015.

[53] M. J. Leyland, M. N. A. Beurskens, L. Frassinetti, C. Giroud, S. Saarelma, P. B. Snyder, J. Flanagan, S. Jachmich, M. Kempenaars, P. Lomas, G. Maddison, R. Neu, I. Nunes, and K. J. Gibson. The h-mode pedestal structure and its role on confinement in jet with a carbon and metal wall. *Nuclear Fusion*, 55(1):013019, 2015.

[54] C.F. Maggi, L. Frassinetti, L. Horvath, A. Lunniss, S. Saarelma, H. Wilson, J. Flanagan, M. Leyland, I. Lupelli, S. Pamela, H. Urano, L. Garzotti, E. Lerche, I. Nunes, F. Rimini, and JET Contributors. Studies of the pedestal structure and inter-elm pedestal evolution in jet with the iter-like wall. *Nuclear Fusion*, 57(11):116012, 2017.

[55] L. Frassinetti, M.N.A. Beurskens, S. Saarelma, J.E. Boom, E. Delabie, J. Flanagan, M. Kempenaars, C. Giroud, P. Lomas, L. Meneses, C.S. Maggi, S. Menmuir, I. Nunes, F. Rimini, E. Stefanikova, H. Urano, G. Verdoolaege, and JET Contributors. Global and pedestal confinement and pedestal structure in dimensionless collisionality scans of low-triangularity h-mode plasmas in jet-ilw. *Nuclear Fusion*, 57(1):016012, 2017.

[56] C. P. Perez, H. R. Koslowski, T. C. Hender, P. Smeulders, A. Loarte, P. J. Lomas, G. Saibene, R. Sartori,

M. Becoulet, T. Eich, R. J. Hastie, G. T. A. Huysmans, S. Jachmich, A. Rogister, F. C. Schller, and JET EFDA contributors. Washboard modes as elm-related events in jet. *Plasma Physics and Controlled Fusion*, 46(1):61, 2004.

[57] T Bolzonella, H Zohm, M Maraschek, E Martines, S Saarelma, S Gnter, and ASDEX Upgrade Team. High frequency mhd activity related to type i elms in asdex upgrade. *Plasma Physics and Controlled Fusion*, 46(5A):A143, 2004.

[58] A. Diallo, J. W. Hughes, M. Greenwald, B. LaBombard, E. Davis, S-G. Baek, C. Theiler, P. Snyder, J. Canik, J. Walk, T. Golfinopoulos, J. Terry, M. Churchill, A. Hubbard, M. Porkolab, L. Delgado-Aparicio, M. L. Reinke, A. White, and Alcator C-Mod team. Observation of edge instability limiting the pedestal growth in tokamak plasmas. *Phys. Rev. Lett.*, 112:115001, Mar 2014.

[59] A. Diallo, J.W. Hughes, S-G. Baek, B. LaBombard, J. Terry, I. Cziegler, A. Hubbard, E. Davis, J. Walk, L. Delgado-Aparicio, M.L. Reinke, C. Theiler, R.M. Churchill, E.M. Edlund, J. Canik, P. Snyder, M. Greenwald, A. White, and the Alcator C-Mod Team. Quasi-coherent fluctuations limiting the pedestal growth on alcator c-mod: experiment and modelling. *Nuclear Fusion*, 55(5):053003, 2015.

[60] A. Diallo, R. J. Groebner, T. L. Rhodes, D. J. Battaglia, D. R. Smith, T. H. Osborne, J. M. Canik, W. Guttenfelder, and P. B. Snyder. Correlations between quasi-coherent fluctuations and the pedestal evolution during the inter-edge localized modes phase on diii-d. *Physics of Plasmas*, 22(5):056111, 2015.

[61] A.V. Bogomolov, I.G.J. Classen, J.E. Boom, A.J.H. Donn, E. Wolfrum, R. Fischer, E. Viezzer, P. Schneider, P. Manz, W. Suttrop, and N.C. Luhmann Jr. Study of the elm fluctuation characteristics during the mitigation of type-i elms. *Nuclear Fusion*, 55(8):083018, 2015.

[62] F M Laggner, E Wolfrum, M Cavedon, F Mink, E Viezzer, M G Dunne, P Manz, H Doerk, G Birkenmeier, R Fischer, S Fietz, M Maraschek, M Willensdorfer, F Aumayr, the EUROfusion MST1 Team, and the ASDEX Upgrade Team. High frequency magnetic fluctuations correlated with the inter-elm pedestal evolution in asdex upgrade. *Plasma Physics and Controlled Fusion*, 58(6):065005, 2016.

[63] Felician Mink, Elisabeth Wolfrum, Marc Maraschek, Hartmut Zohm, Lszl Horvth, Florian M Laggner, Peter Manz, Eleonora Viezzer, Ulrich Stroth, and the ASDEX Upgrade Team. Toroidal mode number determination of elm associated phenomena on asdex upgrade. *Plasma Physics and Controlled Fusion*, 58(12):125013, 2016.

[64] T Zhang, X Han, X Gao, H Q Liu, T H Shi, J B Liu, Y Liu, D F Kong, Z X Liu, H Qu, H M Xiang, K N Geng, Y M Wang, F Wen, S B Zhang, B L Ling, and the EAST team. Outward particle transport by coherent mode in the h-mode pedestal in the experimental advanced superconducting tokamak (east). *Plasma Physics and Controlled Fusion*, 59(6):065012, 2017.

[65] W Suttrop, K Bchl, H J de Blank, J Schweinzer, H Zohm, ASDEX Upgrade team, NBI group, and ICRH group. Characteristics of edge localized modes in asdex upgrade. *Plasma Physics and Controlled Fusion*, 38(8):1407, 1996.

[66] C. P. Perez, H. R. Koslowski, G. T. A. Huysmans, T. C. Hender, P. Smeulders, B. Alper, E. de la Luna, R. J. Hastie, L. Meneses, M. F. F. Nave, V. Parail, M. Zerbini, and JET-EFDA Contributors. Type-i elm precursor modes in jet. *Nuclear Fusion*, 44(5):609, 2004.

[67] N. Oyama, N. Hayashi, N. Aiba, A. Isayama, H. Urano, Y. Sakamoto, Y. Kamada, T. Takizuka, and the JT-60 Team. Characteristics and control of the type i edge localized mode in jt-60u. *Nuclear Fusion*, 51(3):033009, 2011.

[68] N. Oyama, N. Asakura, A.V. Chankin, T. Oikawa, M. Sugihara, H. Takenaga, K. Itami, Y. Miura, Y. Kamada, K. Shinohara, and the JT-60 Team. Fast dynamics of type i elms and transport of the elm pulse in jt-60u. *Nuclear Fusion*, 44(5):582, 2004.

[69] Y. Huang, C.H. Liu, L. Nie, Z. Feng, X.Q. Ji, K. Yao, G.L. Zhu, Yi Liu, Z.Y. Cui, L.W. Yan, Q.M. Wang, Q.W. Yang, X.T. Ding, J.Q. Dong, and X.R. Duan. Features of spontaneous and pellet-induced elms on the hl-2a tokamak. *Nuclear Fusion*, 52(11):114008, 2012.

[70] A.F. Mink, M. Hoelzl, E. Wolfrum, F. Orain, M. Dunne, A. Lessig, S. Pamela, P. Manz, M. Maraschek, G.T.A. Huijsmans, M. Becoulet, F.M. Laggner, M. Cavedon, K. Lackner, S. Gnter, U. Stroth, and The ASDEX Upgrade Team. Nonlinear coupling induced toroidal structure of edge localized modes.

Nuclear Fusion, 58(2):026011, 2018.

[71] G. T. A. Huysmans, T. C. Hender, and B. Alper. Identification of external kink modes in jet. *Nuclear Fusion*, 38(2):179, 1998.

[72] E. R. Solano, P. J. Lomas, B. Alper, G. S. Xu, Y. Andrew, G. Arnoux, A. Boboc, L. Barrera, P. Belo, M. N. A. Beurskens, M. Brix, K. Crombe, E. de la Luna, S. Devaux, T. Eich, S. Gerasimov, C. Giroud, D. Harting, D. Howell, A. Huber, G. Kocsis, A. Korotkov, A. Lopez-Fraguas, M. F. F. Nave, E. Rachlew, F. Rimini, S. Saarelma, A. Sirinelli, S. D. Pinches, H. Thomsen, L. Zabeo, and D. Zarzoso. Observation of confined current ribbon in jet plasmas. *Phys. Rev. Lett.*, 104:185003, May 2010.

[73] R. J. Groebner, D. R. Baker, K. H. Burrell, T. N. Carlstrom, J. R. Ferron, P. Gohil, L. L. Lao, T. H. Osborne, D. M. Thomas, W. P. West, J. A. Boedo, R. A. Moyer, G. R. McKee, R. D. Deranian, E. J. Doyle, C. L. Rettig, T. L. Rhodes, and J. C. Rost. Progress in quantifying the edge physics of the hmode regime in diii-d. *Nuclear Fusion*, 41(12):1789, 2001.

[74] L. Frassinetti, M. N. A. Beurskens, R. Scannell, T. H. Osborne, J. Flanagan, M. Kempenaars, M. Maslov, R. Pasqualotto, and M. Walsh. Spatial resolution of the jet thomson scattering system. *Review of Scientific Instruments*, 83(1):013506, 2012.

[75] J. W. Connor, R. J. Hastie, and J. B. Taylor. Shear, periodicity, and plasma ballooning modes. *Phys. Rev. Lett.*, 40:396–399, Feb 1978.

[76] F. L. Hinton and R. D. Hazeltine. *Rev. Mod. Phys.*, 48:239, 1976.

[77] E. A. Belli and J. Candy. Kinetic calculation of neoclassical transport including self-consistent electron and impurity dynamics. *Plasma Physics and Controlled Fusion*, 50(9):095010, 2008.

[78] E. A. Belli and J. Candy. Full linearized fokkerplanck collisions in neoclassical transport simulations. *Plasma Physics and Controlled Fusion*, 54(1):015015, 2012.

[79] O. Sauter, C. Angioni, and Y. R. Lin-Liu. Neoclassical conductivity and bootstrap current formulas for general axisymmetric equilibria and arbitrary collisionality regime. *Physics of Plasmas*, 6(7):2834–2839, 1999.

[80] O. Sauter, C. Angioni, and Y. R. Lin-Liu. Erratum: neoclassical conductivity and bootstrap current formulas for general axisymmetric equilibria and arbitrary collisionality regime [phys. plasmas 6, 2834 (1999)]. *Physics of Plasmas*, 9(12):5140–5140, 2002.

[81] E A Belli, J Candy, O Meneghini, and T H Osborne. Limitations of bootstrap current models. *Plasma Physics and Controlled Fusion*, 56(4):045006, 2014.

[82] G. T. A. Huysmans, J. P. Goedbloed, and W. Kerner. Isoparametric bicubic hermite elements for solution of the grad-shafranov equation. In Armin Tenner, editor, *Proc. CP90 Europhys. Conf. on Comput. Phys.*, Amsterdam, The Netherlands (10-13 September 1990), pages 371–376, Singapore: World Scientific, 1991.

[83] R. Hager and C. S. Chang. Gyrokinetic neoclassical study of the bootstrap current in the tokamak edge pedestal with fully non-linear coulomb collisions. *Physics of Plasmas*, 23(4), 2016.

[84] A. B. Mikhailovskii et al. *Plasma Phys. Rep.*, 23:844, 1997.

[85] J W Connor, C J Ham, and R J Hastie. The effect of plasma beta on high- n ballooning stability at low magnetic shear. *Plasma Physics and Controlled Fusion*, 58(8):085002, 2016.

[86] P. B. Snyder, K. H. Burrell, H. R. Wilson, M. S. Chu, M. E. Fenstermacher, A. W. Leonard, R. A. Moyer, T. H. Osborne, M. Umansky, W. P. West, and X. Q. Xu. Stability and dynamics of the edge pedestal in the low collisionality regime: physics mechanisms for steady-state elm-free operation. *Nuclear Fusion*, 47(8):961, 2007.

[87] Xi Chen, K. H. Burrell, N. M. Ferraro, T. H. Osborne, M. E. Austin, A. M. Garofalo, R. J. Groebner, G. J. Kramer, N. C. Luhmann Jr, G. R. McKee, C. M. Muscatello, R. Nazikian, X. Ren, P. B. Snyder, W. M. Solomon, B. J. Tobias, and Z. Yan. Rotational shear effects on edge harmonic oscillations in diii-d quiescent h-mode discharges. *Nuclear Fusion*, 56(7):076011, 2016.

[88] Xi Chen, K.H. Burrell, T.H. Osborne, W.M. Solomon, K. Barada, A.M. Garofalo, R.J. Groebner, N.C. Luhmann, G.R. McKee, C.M. Muscatello, M. Ono, C.C. Petty, M. Porkolab, T.L. Rhodes, J.C. Rost, P.B. Snyder, G.M. Staebler, B.J. Tobias, Z. Yan, and the DIII-D Team. Stationary qh-mode plasmas with high and wide pedestal at low rotation on diii-d. *Nuclear Fusion*, 57(2):022007, 2017.

[89] Xi Chen, K.H. Burrell, T.H. Osborne, K. Barada, N.M. Ferraro, A.M. Garofalo, R.J. Groebner, G.R. McKee, C.C. Petty, M. Porkolab, T.L. Rhodes, J.C. Rost, P.B. Snyder, W.M. Solomon, Z. Yan, and The DIII-D Team. Bifurcation of quiescent h-mode to a wide pedestal regime in diii-d and advances in the understanding of edge harmonic oscillations. *Nuclear Fusion*, 57(8):086008, 2017.

[90] A. M. Garofalo, K. H. Burrell, D. Eldon, B. A. Grierson, J. M. Hanson, C. Holland, G. T. A. Huijsmans, F. Liu, A. Loarte, O. Meneghini, T. H. Osborne, C. Paz-Soldan, S. P. Smith, P. B. Snyder, W. M. Solomon, A. D. Turnbull, and L. Zeng. The quiescent h-mode regime for high performance edge localized mode-stable operation in future burning plasmas. *Physics of Plasmas*, 22(5):056116, 2015.

[91] H. R. Wilson and S. C. Cowley. Theory for explosive ideal magnetohydrodynamic instabilities in plasmas. *Phys. Rev. Lett.*, 92:175006, Apr 2004.

[92] C. J. Ham, S. C. Cowley, G. Brochard, and H. R. Wilson. Nonlinear stability and saturation of ballooning modes in tokamaks. *Phys. Rev. Lett.*, 116:235001, Jun 2016.